# Versatile Bottom-Up Construction of Diverse Macromolecules on a Surface Observed by Scanning Tunneling Microscopy

**Sam Haq,[†] Felix Hanke,[†,§] John Sharp,[†] Mats Persson,[†] David B. Amabilino,[*,‡,⊥] and Rasmita Raval[*,†]**

[†]Surface Science Research Centre, Department of Chemistry, University of Liverpool, L69 3BX, Liverpool, U.K. and [‡]Institut de Ciència de Materials de Barcelona (ICMAB-CSIC), Campus Universitari, 08193 Bellaterra, Catalonia, Spain. [§]Present address (F.H.): BIOVIA, 334 Science Park, Cambridge, CB4 0WN, U.K. [⊥]Present address (D.B.A.): School of Chemistry, University of Nottingham, NG72RD, Nottingham, U.K.

**ABSTRACT** The heterocoupling of organic building blocks to give complex multicomponent macromolecules directly at a surface holds the key to creating advanced molecular devices. While "on-surface" synthesis with prefunctionalized molecules has recently led to specific one- and two- component products, a central challenge is to discover universal connection strategies that are applicable to a wide range of molecules. Here, we show that direct activation of C—H bonds intrinsic to $\pi$-functional molecules is a highly generic route for connecting different building blocks on a copper surface. Scanning tunneling microscopy (STM) reveals that covalent $\pi$-functional macromolecular heterostructures, displaying diverse compositions, structures and topologies, are created with ease from seven distinct building blocks (including porphyrins, pentacene and perylene). By exploiting differences in C—H bond reactivity in the deposition and heating protocols we also demonstrate controlled synthesis of specific products, such as block copolymers. Further, the symmetry and geometry of the molecules and the surface also play a critical role in determining the outcome of the covalent bond forming reactions. Our "pick-mix-and-link" strategy opens up the capability to generate libraries of multivariate macromolecules directly at a surface, which in conjunction with nanoscale probing techniques could accelerate the discovery of functional interfaces.

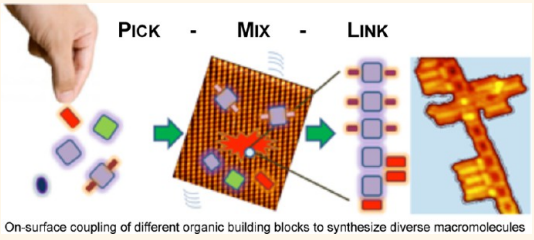

On-surface coupling of different organic building blocks to synthesize diverse macromolecules

**KEYWORDS:** covalent assembly · on-surface synthesis · porphyrins · pentacene · perylene · surface chemistry · C—H bond activation

The formation of a broad mix of multicomponent macromolecules, comprising combinations of simple molecular building blocks, is a key step in generating complexity, diversity and advanced functionality in synthetic materials. In the fields of systems biology and systems chemistry, attaining compositional and topological diversity of macromolecules is fundamental for realizing complex functions.[1] Similarly, introducing macromolecular complexity and diversity directly *at a surface* is a major research challenge in molecular electronics, biomedical devices, sensors, energy harnessing and catalysis.[2−4] An important route to achieve this is *via* covalent heterocoupling of organic building blocks directly on a surface to give multicomponent macromolecules. Recently, "on-surface" synthesis with prefunctionalized molecules has led to specific one- and two-component products with remarkable efficiency.[5−19] While certain specific reactions are known to proceed smoothly on surfaces,[20,21] the discovery of universal connection strategies that are applicable to a wide range of molecules is appealing. Furthermore, a fundamental barrier to bottom-up "on-surface" synthesis of molecular devices is that the macromolecular architectures required to deliver advanced functions are largely unknown. It may, therefore, be timely to switch to scenarios reminiscent of synthetic biology and systems chemistry[1] whereby versatile and highly parallel on-surface coupling of many different molecules yields diverse and complex macromolecules. Each discrete oligomolecular species synthesized at the surface would be defined by its components, the nature of the bonds that link them and their resulting spatial arrangements. Each would represent a different functionality,

* Address correspondence to raval@liv.ac.uk, david.amabilino@nottingham.ac.uk.

Received for review June 14, 2013 and accepted September 5, 2014.

**Published online September 05, 2014**
**10.1021/nn502388u**

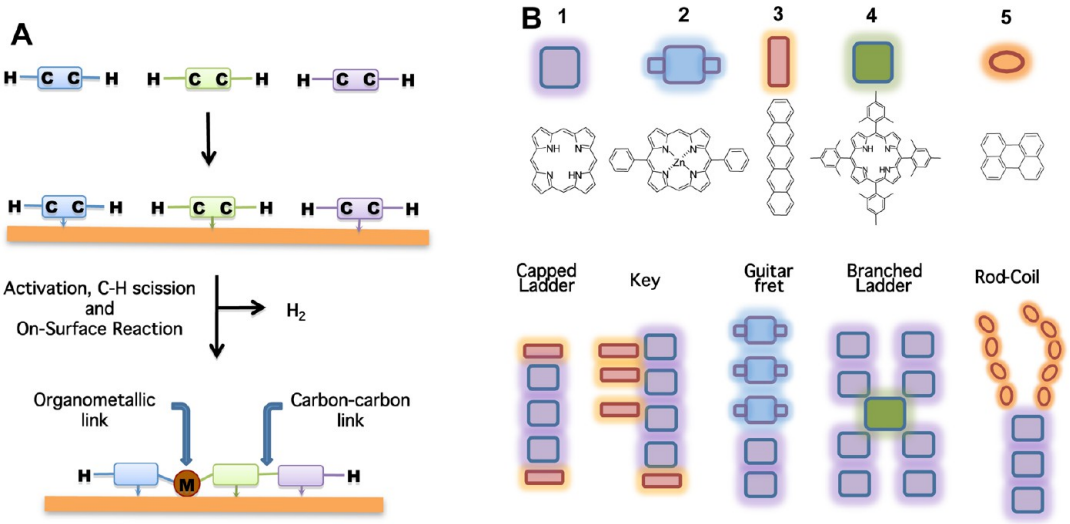


**Figure 1. General overview of individual molecular building blocks and some of the hetero-organic macromolecules created using generic C−H bond activation at a Cu(110) surface. (A) Schematic showing general covalent coupling of organic components at a metal surface *via* C−H activation and formation of C−C and C−Metal−C organometallic bonds. (B) Molecules used in this study: $H_2$-porphyrin (1), Zn(II)diphenylporphyrin (2), pentacene (3), tetramesitylporphyrin (4), and perylene (5), with their associated chemical structures and the simplified schematic representations, which are used to illustrate the range of complex macromolecules formed. Lower part shows examples of individual covalent heterostructures formed on the Cu(110) surface that are observed in this study: capped ladder, key, guitar fret, branched ladder and rod−coil.**

which can eventually be assayed for function by surface nanoscale probing techniques and, thus, could accelerate the discovery of functional interfaces and molecular materials, in an analogous way to combinatorial strategies for drug and materials discovery.[22−24]

Multivariate heterostructures could, in principle, be generated at surfaces using specifically prefunctionalized molecules; however, this can require significant synthetic effort to create the requisite molecular building blocks. We, therefore, have pursued an alternative route by exploiting surface reactivity to directly activate C−H bonds that are ubiquitous in organic building blocks. Thus, we have previously linked porphyrins together at the Cu(110) surface *via* C−H scission followed by either direct C−C[25] or C−metal−C bond[26,27] formation. During these processes, metalation of the porphyrin can also occur, in itself an interesting process.[25−29] Here, we establish the wider generality of using the C−H group as an effective synthon and show that the direct activation of C−H bonds intrinsic to organic molecules is a highly generic route for connecting many organic components on a copper surface (Figure 1). Implementation of this general approach to multicomponent systems is nontrivial because the relative rates of reactions and bond formation of the different components may not enable cross-coupling to take place. The development of this new surface chemistry has direct parallels in the related contemporary challenges of C−H bond activation[30] and carbon metathesis[31] for chemical synthesis and heterogeneous catalysis.

The functional units used here, namely, pentacene, perylene, and different porphyrins (Figure 1), are successfully employed in molecular electronics and organic semiconductors.[32] Further, oligomers of porphyrins, perylenes and pentacene are attracting interest for their potential in molecular wires, organic semiconductors, light harvesting and catalytic applications.[32] The components we have chosen have different sizes, symmetries and geometries, allowing easy identification by scanning tunneling microscopy (STM) so that the molecular constitution of each covalently linked heterostructure can be mapped together with the regioselectivity of the reaction that produces it. These molecular building blocks also possess different types of C−H bonds: pentacene and perylene possess $sp^2$ hybridized carbon atoms only, while porphyrins can have porphyrinyl, phenyl or methyl moieties, with $sp^2$ and $sp^3$ hybridized carbon atoms. We show that each component can react in a number of different ways, and combinations of components lead to the highly varied topologies and $\pi$-functional macromolecular heterostructures shown schematically in Figure 1. Some of these structures are familiar from polymer syntheses, such as the branched ladder, or the rod−coil, but other combinations such as the "capped ladder" and the "key" are quite unique outputs of selective surface chemistry and represent new classes of macromolecular entities that have no counterpart in homogeneous organic synthesis. By exploiting differences in C−H bond reactivity in the deposition and heating protocols we also demonstrate controlled synthesis of specific products such as block polymers, visually similar to a "guitar fret", Figure 1.

## RESULTS AND DISCUSSION

**1D Oriented Random and Block Copolymers of Porphyrins.** Porphyrins are a functional unit that can be used for

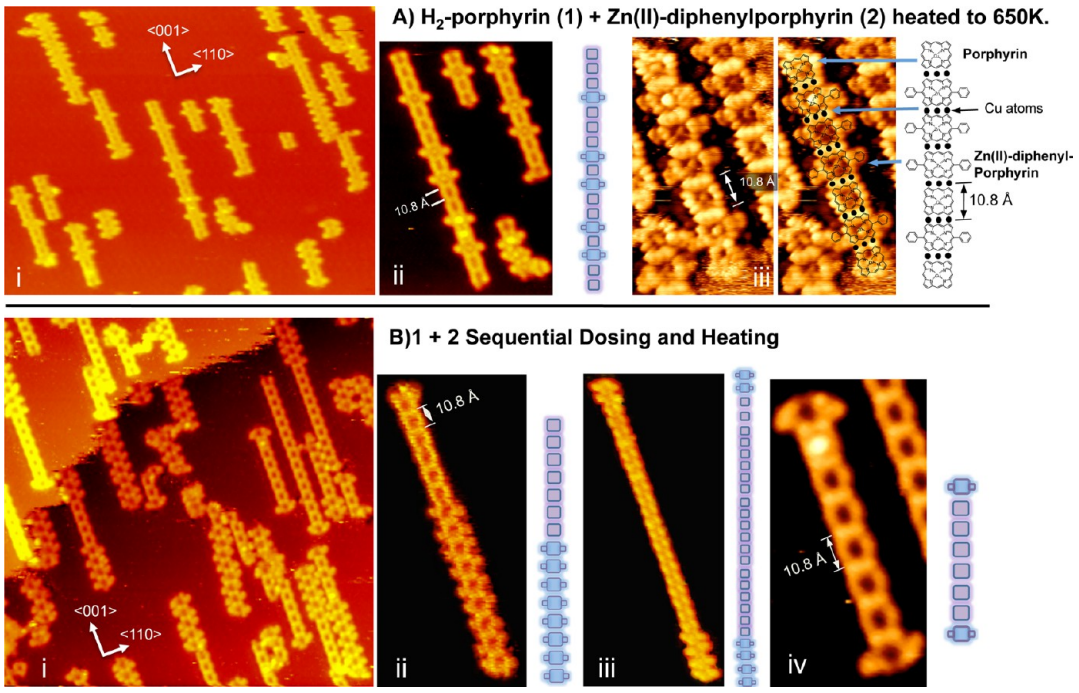


**Figure 2. The creation of diverse covalently bonded linear oligomers *via* reaction of $H_2$-porphyrin (1) with Zn(II)-diphenylporphyrin (2) on Cu(110). (A) STM images obtained after both 1 and 2 are coadsorbed at 300 K and heated to 650 K. (i) Large area image showing a range of products: 335 × 270 Å$^2$, $I_t$ = 0.15 nA, $V_t$ = −1.27 V; (ii) detail of a random copolymer: 100 × 190 Å$^2$, $I_t$ = 0.13 nA, $V_t$ = −1.68 V; (iii) high resolution STM image of a copolymer chain showing the Cu atoms forming organometallic linkages: 35 × 70 Å$^2$, $I_t$ = 0.17 nA, $V_t$ = −0.83 V. (B) STM images obtained following a sequential reaction protocol, in which (1) was dosed first, reacted at 650 K to form chains, followed by adsorption of (2) and heating to 560 K. (i) Large area image, 300 × 300 Å$^2$, $I_t$ = 0.07 nA, $V_t$ = −1.1 V; (ii) "guitar-fret" block copolymer structure, 65 × 170 Å$^2$, $I_t$ = 0.14 nA, $V_t$ = −0.57 V; (iii) multiply capped block polymer structure 90 × 265 Å$^2$, $I_t$ = 0.15 nA, $V_t$ = −0.45 V; (iv) singly capped polymer structure, 40 × 85 Å$^2$, $I_t$ = 0.06 nA, $V_t$ = −1.10 V.**

applications ranging from catalysis, oxygen-transport, charge transport to data storage. Oligomers of porphyrins are attracting interest as molecular wires and for light harvesting applications[32] and there is considerable interest in coupling different types of porphyrins together in order to increase both tuneability and range of function. As a first step toward creating such systems at a surface, we investigated the creation of porphyrin copolymers on Cu(110) using monomers of 2*H*-porphyrin (**1**) and Zn(II)-diphenylporphyrin (**2**), Figure 2.

In order to understand this copolymer system, it is useful to first draw comparison with the homopolymer systems. We have established previously, *via* detailed STM and periodic DFT calculations, that that each component alone can homocouple to generate 1D organocopper homopolymers[26] *via* edge-to-edge porphyrin−Cu−porphyrin connections where cleavage of the $sp^2$ C−H bond occurs at the 3, 5, and 7 positions and leads to formation of one, two or three C−Cu−C bonds, Figure 3. During the heating process, metalation of the 2*H*-porphyrin (**1**) also takes place,[26] in which N−H bonds are broken and Cu inserted into the center of the porphyrin ring. Further, we have previously shown that both homopolymers of **1** and **2** grow preferentially along the [001] surface direction, as a result of the geometry-match of the macromolecule with the underlying surface,[27] as depicted in Figure 3A. Figure 3A(i) summarizes the calculated structure of the oriented homopolymer of **1,** its registry and preferential orientation with the underlying surface, and the C−Cu−C organometallic connections that drive this assembly, as deduced from our previous experimental STM, periodic DFT and simulated STM data.[26,27] Calculated structures for both the two Cu- and three Cu-connected homopolymers are shown, Figure 3A and B, along with simulated STM data and experimental data obtained on this system. There is excellent agreement between the simulated and experimental STM data, with both demonstrating that individual porphyrin **1** units can be identified by STM, along with the connecting Cu atoms, which give rise to signature bright spots - each spot corresponds to one inserted Cu atom, Figure 3A,B. Specifically, the 10.8 Å distance between porphyrin cores is consistent with the calculated distance between porphyrin **1** components connected *via* organometallic C−Cu−C bonds. In this structure, the C−Cu−C bonds are stabilized by the close commensurability with the underlying surface that provides a good match between the monomer−monomer distance and the organometallic linkage, while also accommodating the connecting Cu atom at energetically favored 4-fold hollow sites between the close-packed rows.[26,27]

Here, we create a co-oligomer by coadsorbing porphyrins **1** and **2** on the Cu(110) surface at room

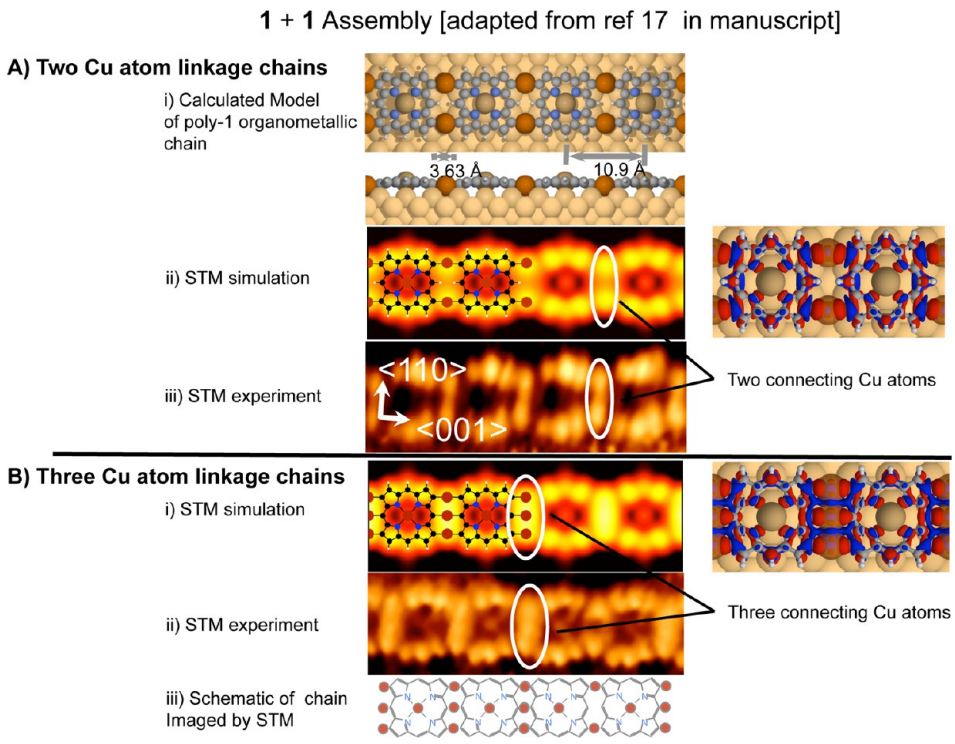


**Figure 3. The nature of the Cu−porphyrin chain formed at the surface with 2 and 3 Cu adatom connection. (A) (i) Computed geometric structure of the Cu−porphyrin chain with a 2 Cu atom connection presenting top- and side-views showing the length scale and the bending of the porphyrin macrocycle toward the two connecting Cu atoms; (ii) simulated STM images (4.36 nm × 1.54 nm, $V_{tip}$ = −0.1 V) and (iii) experimental STM image 4.45 nm × 1.4 nm ($V_t$ = +0.4 V, $I_t$ = 0.42 nA) showing submolecular detail of a 2 Cu atom coupled Cu−porphyrin nanowire. (B) (i) Simulated STM images (4.36 nm × 1.54 nm, $V_{tip}$ = −0.1 V) of a Cu−porphyrin nanowire with a 3 Cu atom connection. (ii) Experimental STM image 4.60 nm × 1.4 nm ($V_t$ = −0.76 V, $I_t$ = 0.19 nA) showing submolecular detail of a Cu−porphyrin nanowire with predominantly 3 Cu atom connections and one 2 Cu atom connection. (iii) Schematic representation identifying each connection. Two images to the right of the STM data are calculated electron density differences for the 2 and 3 Cu atom connections, respectively, indicating the bonding mechanisms for the C−Cu−C connection and the Cu−porphyrin−substrate interaction. The electron density difference is taken between the adsorbed system and the bare surface. Red and blue correspond to electron accumulation and depletion, respectively. Note that the connecting Cu atoms are partially transparent for clarity.**

temperature and then heating to 650 K. STM images (Figure 2A) show that the two components indeed link together to form unidirectional linear co-oligomers. Individual monomers within each surface-synthesized oligomer can be resolved by STM, with **1** producing square images with straight edges, while **2** displays the phenyl groups, giving a serrated appearance along the polymer length. Figure 2A(i,ii) show that for the codeposited system, the monomer components **1** and **2** appear to be incorporated into the macromolecules in a random way, characteristic of the result expected in a bulk polymerization. Thus, a wide variety of random co-oligomers (Figure 2A(i,ii)) are produced. High resolution STM images, Figure 2A(iii), confirm that the organometallic linkage is also employed in the copolymer, with the connecting metal atoms clearly imaged as bright spots, and the individual units separated by the expected distance[26] of 10.8 Å (Figures 2, 3), as discussed above. The defined orientation of the copolymers shown in Figure 2 is in keeping with the behavior previously observed for the homopolymer of **1**,[26,27,33] and arises because the identical molecular cores of the copolymer and the resulting C−Cu−C linkages are subject to the same commensurability with the underlying surface, and drive copolymer synthesis along the [001] direction. This specific coupling direction means that lateral positions of the macrocycle aligned along the [1$\bar{1}$0] directions remain available to locate other functional groups, thus allowing compositional variation to be introduced.

The "mix-and-heat" experiment above generates an enormous diversity of random copolymers. However, the reaction output can be controlled by exploiting differences in the C−H group reactivity of the two components. Specifically, Zn(II)-diphenylporphyrin **2** reacts at a much lower temperature of 560 K compared to 650 K for porphyrin **1**. Thus, the sequence of connectivity can be tailored to predispose the system toward block copolymer creation, in which a section derived from one porphyrin is followed by a section composed of the other. Hence, porphyrin **1** was first adsorbed at the surface and heated to 650 K to link the like components together. This was followed by adsorption of **2** and heating to the lower temperature of 560 K, where only **2**−**2** or **2**−**1** porphyrin connections can be made, while **1**−**1** are inaccessible. This altered

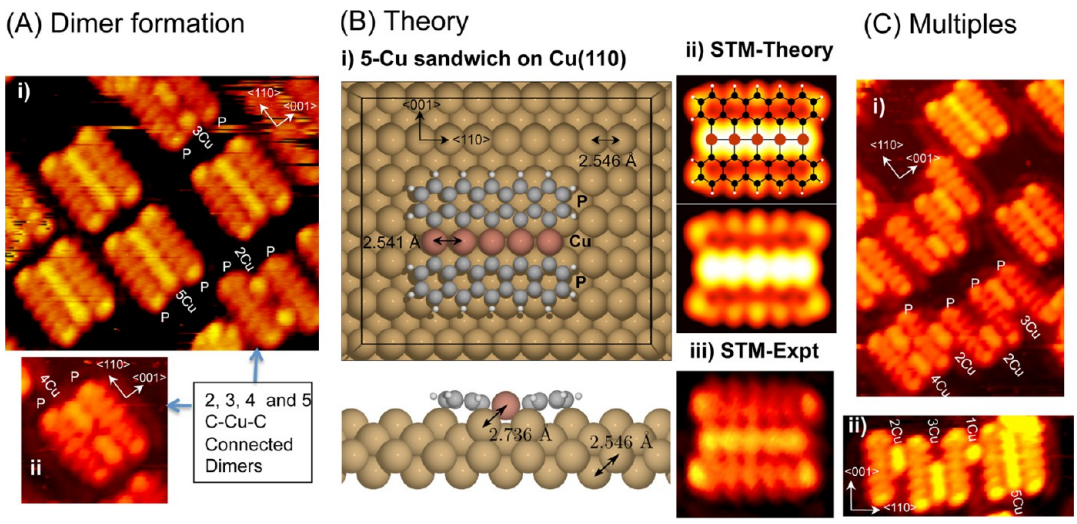


**Figure 4. The creation of pentacene sandwich structures on Cu(110). (A) STM images showing dimer formation, obtained after pentacene (3) adsorbed at 300 K and heated to 600 K. (i,ii) images showing dimers with different number of reacted Cu atoms: (i) 50 × 40 Å$^2$, $I_t$ = 0.21 nA, $V_t$ = −0.04 V; (ii) selected pentacene dimer showing 4-Cu atom sandwich structure, $I_t$ = 0.21 nA, $V_t$ = −0.04 V. (B) Theoretical calculations (i) showing optimized geometry of 5-Cu atom pentance sandwich structure on Cu(110). (ii) Theoretically calculated STM image of 5-Cu atom pentacene sandwich structure, $V_t$ = −1.1 V; (iii) experimental STM of 5-Cu atom pentacene sandwich, $I_t$ = 0.19 nA, $V_t$ = −0.034 V. (C) Experimental STM images of multiple pentacene molecules connected by Cu atoms. (i) 40 × 60 Å$^2$, $I_t$ = 0.21 nA, $V_t$ = −0.04 V; (ii) 40 × 20 Å$^2$, $I_t$ = 0.21 nA, $V_t$ = −0.04 V.**

synthesis protocol produces a different distribution of heterostructures in which "guitar fret" block copolymers and capped structures are favored, Figure 2B(ii) and Figure 2B(iii,iv), respectively. In the former, blocks containing a series of porphyrin **1** monomers coupled together are followed by a discrete section of porphyrin **2** monomers. For the capped structures, rods composed only of porphyrin **1** are capped at the end by a single monomer of porphyrin **2**, with capping observed either at one end (single-capped structures) or at both ends (double-capped structures). Again, the STM images allow the spatial distributions of the two components to be mapped within each block copolymer, with the organometallic linkage evidenced by the signature intercomponent distance of 10.8 Å, Figure 2B. Thus, the inherent difference in C−H bond reactivity for the two different molecules opens up a route to selective block copolymer growth without recourse to synthesizing specifically functionalized precursors. In 3D, block copolymers are known to possess different properties compared to random copolymers; thus, the ability to construct block copolymer sequences at surfaces is of potential value. Here, we have shown that depending on the order of deposition and heating, either random or block copolymers incorporating both **1** and **2** monomers are produced with a highly defined orientation with respect to the surface. Such linear co-oligomers of porphyrins are unique.

**Connecting Arenes.** Next, we investigated the behavior of pentacene (**3**) to establish whether C−H activated coupling could be extended to $\pi$-functional hydrocarbons. Pentacene based dimers and oligomers are recently attracting interest for organic semiconductor and photoconductive applications,[34] and it is of interest to explore whether this molecule can be directly coupled together at a surface. The pentacene molecule was first deposited at submonolayer coverage onto Cu(110) at 300 K and then heated to 600 K. Prior to the heating treatment, pentacene diffuses rapidly on the surface and is difficult to image at 300 K (Supporting Information, Figure S1), as has also been reported previously.[35] DFT calculations show that pentacene on Cu(110) has a strong preference for adsorbing with its molecular long axis aligned along the [1$\bar{1}$0] surface direction, and centered over the hollow trough between the close-packed rows.[36]

Following heating to 600 K, our STM images show the formation of discrete dimer sandwich structures, which are now immobile and can be imaged clearly, showing two pentacene molecules joined side-by-side lengthwise and parallel with each other, Figure 4. Notably, discrete bright spots are imaged in between the molecules, Figure 4A(i). This behavior is very different to anything observed at lower temperatures. For example, even when a densely packed periodic pentacene overlayer is created on Cu(110) at 300 K,[35] the pentacenes are only imaged as individual molecules; neither the bright features between adjacent molecules nor the formation of discrete dimer structures is observed. The bright spots imaged in between the molecules are a strong indicator of C−Cu−C connections, with up to five Cu atoms incorporated to create the dimer sandwich, Figure 4A. To assess the creation of organometallic dimer sandwiches, density functional calculations were undertaken for gas phase copper-bridged pentacene dimers, which show that the addition of each Cu atom to create the organometallic C−Cu

bond corresponds to a gain of approximately 0.5 eV (Supporting Information, Figure S2). The 5-Cu bonded dimer sandwich yields an energy gain of over 3 eV associated with the breaking of all five C−H bonds along the length of the pentacene molecule and formation of five C−Cu−C linkages (Supporting Information, Figure S2(ii)). The five connecting Cu atoms in the gas phase dimer are held 2.44 Å apart, which closely matches the Cu−Cu distance (2.5 Å) in the [1$\bar{1}$0] surface direction; this would enable their easy accommodation on the surface as a local "added row" structure.[26,27] This situation would orientate the pentacene long-axis parallel to the Cu(110) rows, which agrees with our STM observation, Figure 4A.

To investigate this further, the adsorption of the five Cu-connected pentacene dimer adsorbed on the Cu(110) surface was studied using plane-wave DFT calculations. DFT calculations confirm that the two coupled pentacene molecules each adsorb at their preferred site positioned between the surface rows[36] with their molecular long axes aligned with the [1$\bar{1}$0] surface direction. Further, the dimensions of the connecting C−Cu−C organometallic bonds matches the monomer−monomer distance very well, and also positions the connecting Cu atoms at their preferred 4-fold hollow sites, which begin to form an additional close packed row, as shown in Figure 4B(i). Our calculations show that the distance between the adjacent connecting Cu atoms increases upon adsorption, from a value of 2.44 Å in gas-phase to 2.54 Å, which is very similar to the distance between bulk close packed Cu atoms, 2.55 Å. The nearest neighbor distance between the connecting Cu atoms and the underlying substrate Cu is slightly greater than that of bulk Cu, 2.74 Å, due to interaction between the adsorbed pentacenes and the connecting Cu atoms.

The electronic structure from the plane-wave DFT calculations was used to generate STM simulations under the Tersoff−Hamann approximation, and the result is shown in Figure 4B(ii). There is excellent agreement with the experimental STM fingerprint, Figure 4B(iii), with all the main features reproduced; namely: the connecting Cu atoms are imaged as 5 bright spots, the five lobes corresponding to each pentacene molecule are imaged, and the ends of the pentacene structure appear brighter than the center. This close agreement between theoretical and experimental results indicates that the pentacene molecules can be coupled at the surface *via* organometallic C−Cu−C bonding. Experimental STM data show that dimer coupling can also occur by incorporation of fewer than five Cu atoms, with examples of two, three and four Cu atom dimers imaged in Figure 4A(i,ii).

Multiple sandwich structures can also be created where three or more pentacene molecules are linked together. Figure 4C shows STM images of such structures, where a number of pentacenes are linked together with a variable number of C−Cu−C linkages, with each incorporated Cu atom producing a discrete bright protrusion. The calculated gas phase 3-pentacene sandwich (Supporting Information, Figure S2), shows that there is an energy gain of −5.94 eV for a 3 pentacene-10 Cu trimer.

**Connecting Dissimilar Molecules: Arenes Plus Porphyrins.** Connecting different $\pi$-functional molecules to form macromolecules with areas of relative electron accepting and electron donating character is an important goal in molecular electronics and light harvesting technology. Recently, covalently coupled porphyrin−pentacene systems have been synthesized in solution phase for photovoltaic applications.[34] We, therefore, investigated whether two very different molecules such as porphyrin **1** and pentacene could be coupled directly at a surface. 2*H*-porphyrin **1** and pentacene were coadsorbed on the Cu(110) surface and reacted together by heating to 650 K under low coverage (<0.25 monolayer) conditions. Figure 5A shows that a diversity of macromolecules is formed, with both like−like coupling and like−unlike coupling taking place. Thus, independent pentacene dimers are observed to coexist alongside pentacene-porphyrin **1** entities on the surface. This observation suggests that, in this kind of complex multicomponent system, the local stoichiometry of the combining molecules will influence the outcome of the coupling on the surface. Thus, differing local concentrations will lead to different macromolecular compositions, as has also been noted for other surface coupling systems.[37,38] In addition to the homocoupling products such as homopolymers of **1** and dimer pentacene sandwiches, heterocoupling also occurs whereby pentacene monomers and dimers are connected to porphyrin **1**. The organometallic bonding between pentacene and porphyrins is again characterized by the interconnecting Cu atoms imaging bright. This is exemplified in Figure 5B(i) where half-capped porphyrins show an unconnected porphyrin end (with no bright Cu atoms) and the pentacene capped end with bright Cu atoms imaged in between. In Figure 5A, the area marked **X** shows a homocoupled pentacene dimer alongside a heterocoupled pentacene capped porphyrin chain; the similarity in connection between the two types of species is evident. Figure 5B(ii) shows higher resolution STM data of half-capped and doubly capped porphyrins, which reveal each individual building block and the connecting Cu atoms. Schematics of the heterostructures formed are shown underneath. STM imaging of higher protrusion features between connected molecules is a signature feature of metal coordination, and has been reported extensively in the literature of metal-coordination systems formed at surfaces[39−41] and on-surface synthesized Cu−C−Cu organometallic systems.[26,27,42] This observation is supported by our DFT modeling and STM simulations, as described

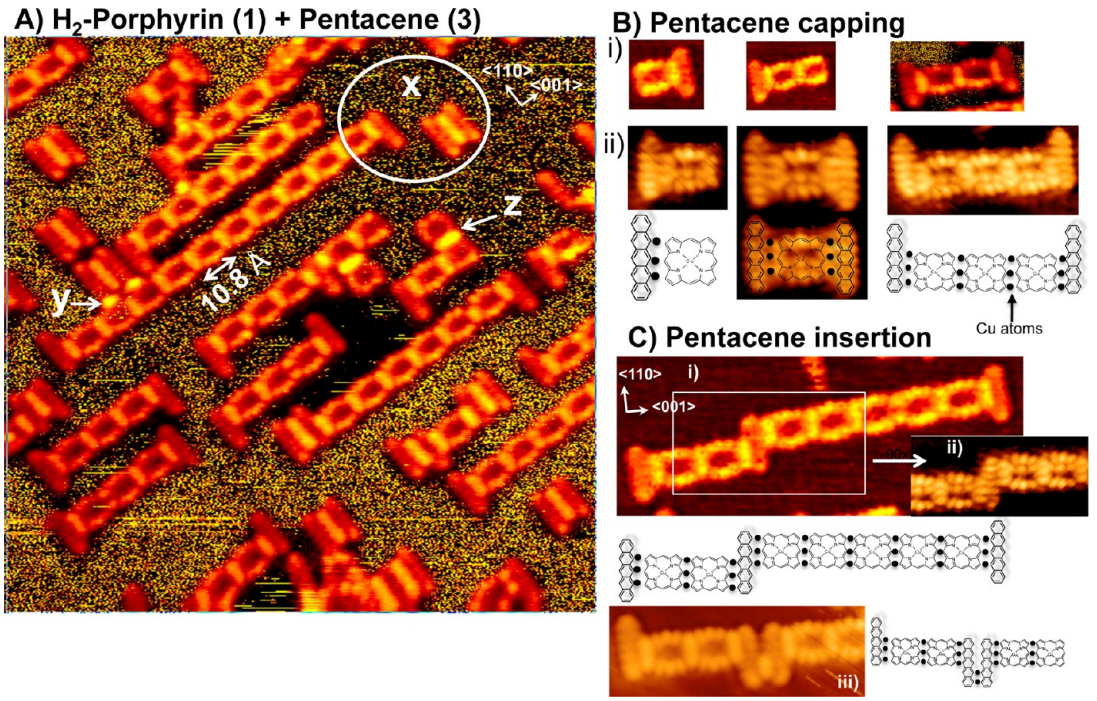


**Figure 5. The creation of macromolecules by reaction of porphyrin and pentacene on Cu(110). STM images and selected schematics of macromolecular structures. (A) STM image showing macromolecule formation after porphyrin (1) and pentacene (3) are coadsorbed at 300 K and heated to 650 K: 150 × 150 Å, $I_t$ = 1.35 nA, $V_t$ = 0.478 V. (B) Selection of reacted porphyrin−Cu−pentacene structures showing pentacene capping at one or both ends of porphyrin. (i) Left to right: $I_t$ = 0.62 nA, $V_t$ = −0.028 V; $I_t$ = 0.62 nA, $V_t$ = −0.028; $I_t$ = 1.35 nA, $V_t$ = 0.478 V. (ii) High resolution images showing details of porphyrin−Cu−pentacene bonding, all three images measured at $I_t$ = 0.19 nA, $V_t$ = −0.01 V. (C) STM images showing pentacene sandwiched between porphyrin chains, (i) 90 × 35 Å, $I_t$ = 0.62 nA, $V_t$ = 0.028 V. (ii) High resolution image showing three Cu atoms on each side of pentacene; $I_t$ = 0.21 nA, $V_t$ = −0.01 V. (iii) Image showing two pentacenes sandwiched between porphyrins; 55 x20 Å, $I_t$ = 0.52 nA, $V_t$ = 0.078 V.**

for the porphyrin and pentacene systems in the preceding sections.

The mixed porphyrin **1**−pentacene system displays modular construction behavior in which dimer and monomer pentacene modules bind to the 1D porphyrin organometallic chains, Figure 5A. Intermodule connections were observed at three positions. First, pentacene monomer and dimer attachment at the porphyrin chain ends occurs to give capped ladder topologies, Figure 5A,B. Second, pentacene can be incorporated in the middle of an oligoporphyrin chain to produce random copolymers, which can have linear or kinked topologies depending on the juxtaposition of the porphyrin chains connected either side of a pentacene connector, Figure 5A,C. For both the capped and inserted configurations, there is a good geometrical fit between porphyrin **1** and pentacene at the surface, with up to three linker Cu atoms able to be accommodated in their preferred "added row" positions. This geometrical aspect could foreseeably be used to couple other aromatic structures to the porphyrin and pentacene units in this setting. The unique structures formed here also demonstrate how other related systems incorporating analogous $\pi$-functional units might be accessible. Third, the pentacene ends can also attach at the side of the oligoporphyrin long edge to produce key topologies, Figure 5A (marked y), forged by organometallic connections. This coupling arrangement is similar to that formed when oligomers of porphyrin **1** attach side-on to give nanoribbons,[26,27] as exemplified in Figure 5A (marked **z**) where an individual porphyrin is coupled side-on to a porphyrin **1** oligomer. It would appear that pentacene can also access a similar bonding configuration, with gas phase DFT calculations showing that C−H bond breaking and copper insertion at the ends of the pentacene molecule is also energetically favorable, (Supporting Information, Figure S2). However, as Hanke *et al.*[27] have demonstrated, the porphyrin side-to-side attachment is stressed due to the poorer geometric fit of the molecular components and the linking Cu atoms with the underlying surface; this leads to preferential covalent coupling at chain ends to propagate 1D rods as opposed to sideways coupling to produce nanoribbons. Similarly, the fit for the pentacene−Cu−porphyrin coupled nanostructure with respect to the underlying surface is poorer in the side-on arrangements, and is observed less often than the capped and inserted configurations. Finally, at high coverages, complex networks form in which pentacene trimers, dimers and monomers are coupled with porphyrin monomers and oligomers *via* Cu atoms, enabling connectivity along many different directions (Supporting Information, Figure S3).

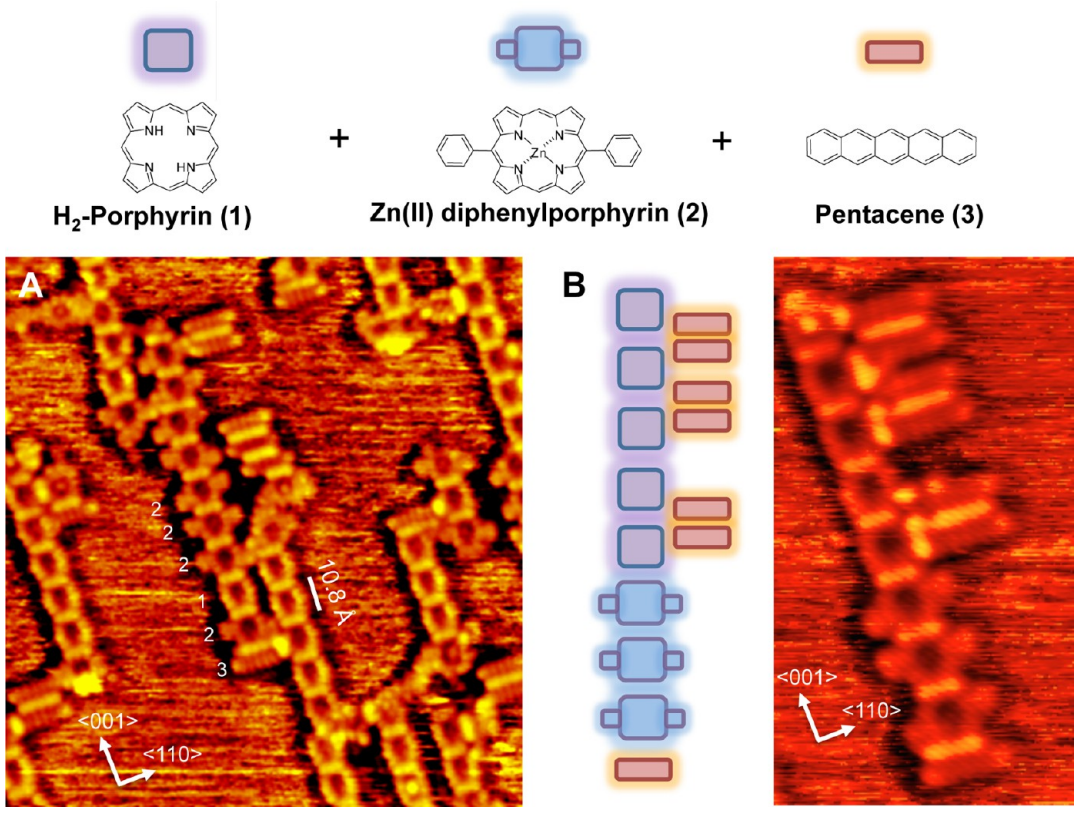


**Figure 6. Three-component heterostructures formed by sequential reactions of $H_2$-porphyrin (1), Zn(II)diphenylporphyrin (2) and pentacene (3). (A) Large area STM image (150 × 160 Å$^2$, $I_t$ = 0.57 nA, $V_t$ = +0.34 V) obtained following a sequential reaction protocol, in which (1) was dosed first and reacted at 650 K to form chains, followed by adsorption of (2) and heating to 650 K to make copolymers, followed by adsorption of (3) and heating to 650 K. Complex three-component macromolecular structures are observed, with bright protrusions between components revealing organometallic linkages *via* coupling Cu atoms. (B) Schematic and STM image of a 3-component key structure: 53 × 90 Å$^2$, $I_t$ = 0.38 nA, $V_t$ = +0.35 V.**

*Three Component Heterostructures.* The C−H synthon is ubiquitous and its surface activation to promote C−H bond breaking and, subsequently, drive intermolecular couplings provides the opportunity to connect many different molecular building blocks together. We demonstrate this capability by generating three-component heterostructures that exploit the different connectivity preferences of the molecular components used up to this point. The reaction of porphyrins **1** and **2** was first coupled sequentially to give 1-D block copolymer chains, and subsequent reaction of pentacene **3** leads to its attachment at the end or the side of the chain, to give capped and key structures, and more complex interchain connections, Figure 6. The detail of a three-component key is shown in Figure 6B, with pentacene attached to the side of porphyrin **1** components in the mixed chain and capping porphyrin **2** at the chain end. As for the pentacene + porphyrin **1** systems, the intermolecular connections are organometallic, with the connecting Cu atoms imaging bright, Figure 6. Importantly, our 3-component system generates a diversity of three component macromolecular structures that are at present inaccessible by any other solution-based protocol. Furthermore, this provides proof-of-principle that, theoretically, there is no upper limit to how many different components can be coupled at a surface using our generic method.

*Creating Further Complex Bicomponent Topologies.* We further extended our repertoire of connections by connecting different topologies (rods, branched networks, coils) together. Porphyrin **1** is an excellent rod-former, Figure 2, and our aim was to link these C−Cu−C coupled rods to branches and coils created by other molecular building blocks.

Branched connectivity is provided by tetramesitylporphyrin (**4**) where we have previously shown[25] that surface activation of the methyl group at the *para* position of the benzene with respect to the porphyrin generates a $CH_2^{\bullet}$ radical group that homocouples the porphyrins *via* C−C covalent links. Since the molecule adopts a specific adsorption geometry at the surface, the 4-methyl groups and, thus, the C−C links are directed along specific diagonal directions. A monomer of porphyrin **4** can couple to another monomer at any of its four corners, naturally leading to branched topologies. The average core-to-core distance between homocoupled tetramesitylporphyrin (**4**) molecules is about 18.8 Å, and agrees with the 19 Å distance calculated if an ethylene ($CH_2$−$CH_2$) linkage is made.[25] Thus, four C−C connections can

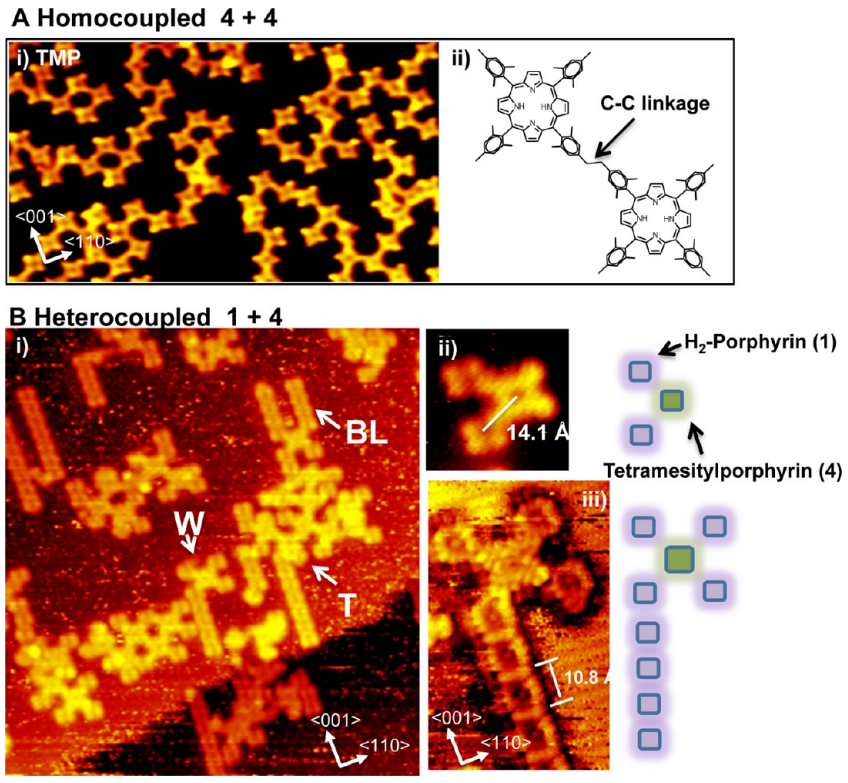


**Figure 7. The creation of diverse C−C covalently bonded oligomers *via* reaction of porphyrins on Cu(110) *via* homo- and hetrocoupling. (A) (i) STM image after tetramesitylporphyrin (TMP) heated to 575 K on Cu(110): 275 × 150 Å$^2$, $I_t$ = 0.18 nA, $V_t$ = −0.32 V. Measured in our previous work, ref 25. (ii) Chemical structure showing covalent bonding between TMP molecules. (B) Creation of rod−branch macromolecules by initially reacting $H_2$-porphyrin (1) to 615 K to form chains and subsequently dosing TMP (4) and heating to 595 K. (i) Large area STM image 300 × 324 Å$^2$, $I_t$ = 0.18 nA, $V_t$ = −1.28 V. (ii) Selected macromolecule showing single TMP (4) covalently bonded to two $H_2$-porphyrin (1) molecules: $I_t$ = 0.24 nA, $V_t$ = −0.78 V. (iii) Small area STM showing a windmill structure: 42 × 76 Å$^2$, $I_t$ = 0.18 nA, $V_t$ = −1.28 V.**

potentially be forged by **4**, at each mesityl group, leading to branched covalent nanostructures, Figure 7A. In this geometry, the distance between the monomers is short enough to enable a C−C bond at the diagonal position to be formed with both porphyrin **4** entities continuing to occupy their preferred adsorption sites. The organometallic link is not formed in this case, presumably, because the positioning of the monomers is not conducive for stabilizing the C−Cu−C bond, either in terms of the bridging distance or the positioning of the connecting Cu atom at a suitable surface site.

In order to create combined rod-branch topologies, porphyrins **1** and **4** are reacted by codeposition at room temperature and heating to 605 K. Figure 7B shows that a range of complex bicomponent structures are generated in which **1** is connected to the corners of **4**. For example, when a building block of **4** reacts with two units of **1**, a two-leaf clover structure is generated, as seen in Figure 7B(ii). Similarly, three-leaf and four-leaf clover structures can also be created. Modular connectivity is also observed when rod and branched topologies further link together to give windmills (W), trees (T) and branched ladders (BL), as seen in Figure 7B(i,iii). The creation of branched-ladder (BL) macromolecules, where chains of **1** grow away from different methyl groups of **4**, indicate that **4** is a suitable linker for the rod structures. In contrast to the examples described previously, it is difficult to identify the exact nature of the bond between these two molecular components from STM data. However, the geometry and dimensions of the resulting structures indicate a covalent C−C linkage resulting from the reaction of the mesityl methylene group of **4** and a pyrrole ring of **1**. This would position **1** at the corners of **4**, as seen in Figure 7B. Further, the center-to-center distance measured between connected porphyrin cores of **1** and **4** ranges from 13.0 to 14.9 Å (with an average of 14.0 Å). When the uncoupled molecules are positioned in their preferred adsorption sites in a geometry closest to the observed one, the core-to-core distance of 15.8 Å is considerably longer than the measured distances. Any organometallic link would result in a longer porphyrin center-to-center distance of the order of 17 Å and, therefore, can be ruled out.

The rod-branched topology formed by the reaction of porphyrin **1** and porphyrin **4** was not observed in any of the other coupling reactions observed in this paper, and shows how specific chemical reactivity can lead to novel structures that are comparable to branched polymers formed in solution. The difference with solution chemistry is the novel coupling route and the fact that both the branching points and the linear

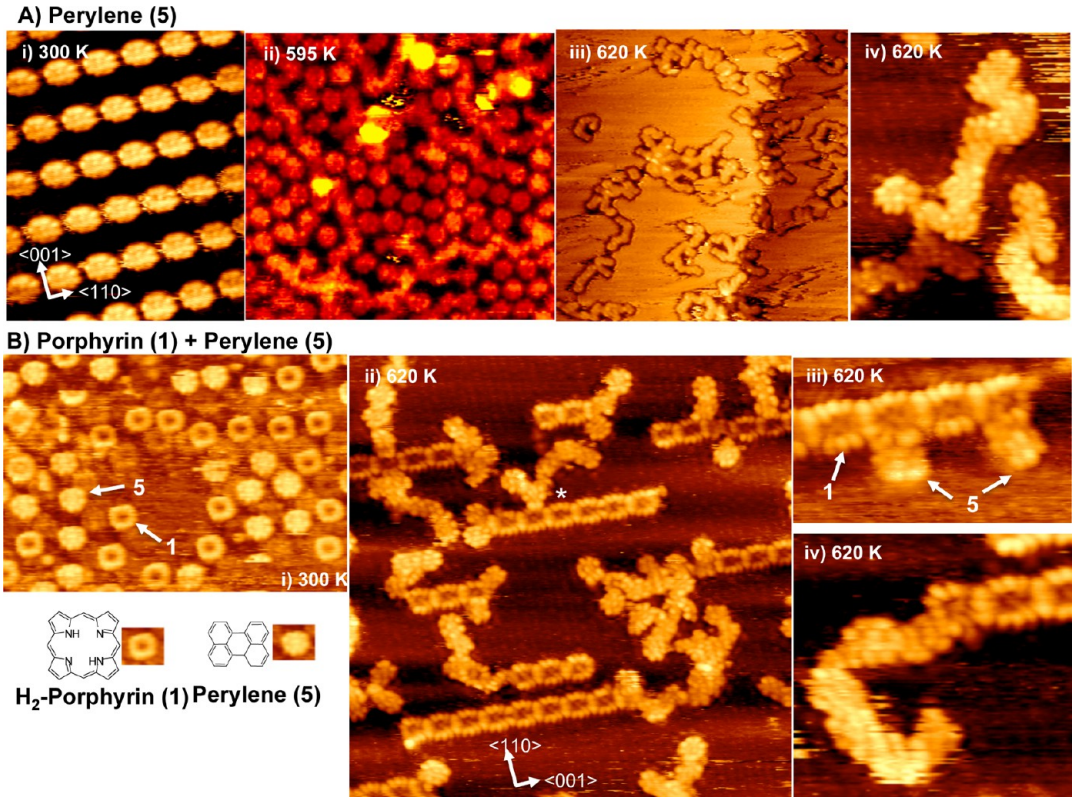


**Figure 8. The creation of covalently bonded oligomers *via* reaction of perylene (5) and porphyrins (1) on Cu(110). (A) STM images of perylene adsorption and reaction on Cu(110). (i) Ordered perylene at 300 K: 85 × 110 Å$^2$, $I_t$ = 0.10 nA, $V_t$ = −0.63 V. (ii) After partial reaction by heating to 595 K: 140 × 140 Å$^2$, $I_t$ = 0.13 nA, $V_t$ = −0.27 V. (iii) Completely reacted perylene after heating to 620 K forming random chains: 300 × 300 Å$^2$, $I_t$ = 0.08 nA, $V_t$ = −0.63 V. (iv) High resolution image showing submolecular structure within a chain: 75 × 50 Å$^2$, $I_t$ = 0.19A, $V_t$ = −0.12 V. (B) STM images showing reaction of porphyrin and perylene (i) after coadsorption at 300 K: 120 × 90 Å$^2$, $I_t$ = 0.39 nA, $V_t$ = 0.15 V; (ii) after reaction by heating to 620 K: 150 × 150 Å$^2$, $I_t$ = 0.20 nA, $V_t$ = −0.11 V. (iii) Selected area showing perylene covalently bonded to side of porphyrin chain: 53 × 30 Å$^2$, $I_t$ = 0.20 nA, $V_t$ = −0.03 V. (iv) Selected area showing coiled perylene chain bonded to end of porphyrin chain: 45 × 45 Å$^2$, $I_t$ = 0.21 nA, $V_t$ = −0.03 V.**

sections of the copolymer are oriented along specific substrate symmetry axes. This feature is once again the result of the geometric match between the surface and the chemical structure of the product. In addition, the resulting surface-based rod-branched macromolecules contain both organometallic bonds (between homocoupled units of **1**) and covalent carbon−carbon bonds (between homocoupled units of **4** and between heterocoupled units of **4** and **1**) in the same structure, highlighting the specificity of the linking reactions.

We also investigated coupling between porphyrin **1** and perylene in order to investigate whether other types of topologies can be coupled at a surface. Porphyrin−perylene dimers and oligomers are also of interest for dye-sensitized solar cells, where the addition of the perylene increases efficiency of light harvesting in spectral regions that are inaccessible by the porphyrin.[43] In contrast to all the systems described above, a very different topology is created when perylene (**5**) is homocoupled on the surface by deposition of a submonolayer on the Cu(110) surface at room temperature and subsequent heating. Perylene adsorption on Cu(110) at 300 K and gently annealing to 370 K leads to organized overlayer phases, with the molecules imaging as discrete entities in the STM data, Figure 8A(i), in accordance with previously published STM data of this system.[44] Distinctive submolecular features are associated with each individual molecule, giving a flower-like STM image. The shortest core-to-core distance between neighboring molecules in this self-assembled phase is 12.5 Å. After heating to 595 K, discrete perylene molecules can be seen to coexist with oligomeric structures, Figure 8A(ii). The oligomeric phase is more cleanly captured when a low coverage of perylene is deposited on the surface and then heated to 610 K, forming a random coil structure, Figure 8A(iii). Random coil oligomer formation has been similarly imaged for a number of systems, including polyimide formation,[7] and oligomerization *via* dehydrogenation of heteroaromatics.[45] We find this topology is also displayed when rubrene and coronene are homocoupled at this surface, where multiple connections lead to distinctive branched and coiled structure (Supporting Information, Figure S4). Higher resolution STM data of the perylene oligomer phase, Figure 8A(iv), show that though the submolecular features of perylene are still discernible, it is difficult to clearly identify each repeating residue on the coiled

oligomer because the variable orientations and the close proximity of the perylene units cause the features from individual molecules to conjoin. However, where two and three connected units are captured in flat orientations w.r.t. the surface, we measure core-to-core distances that range from 7.6 to 8.3 Å, which are consistent with C−C linkages. The random coil topology for the oligomers suggests the C−C linkages are randomly positioned with respect to the molecular framework and the underlying surface; that is, C−H activation and bond-breaking is possible at a number of positions on the molecular periphery, which is consistent with the fact that flat-lying perylene on Cu(110) is able to adopt different alignments of the molecular skeleton with respect to the underlying surface.[44] Thus, a range of monomer-to-monomer approaches suitable for C−C coupling are possible, which leads to diverse macromolecular architectures, whose geometry on the underlying surface is not prescribed, in contrast to all the other examples shown above.

When 2*H*-porphyrin (**1**) and perylene (**5**) are coadsorbed on the surface at 300 K, the individual molecules can be identified, with (**1**) imaging as hollow squares and (**5**) imaging as a flower-like structure, Figure 8B(i). At 300 K, the two molecular components stay apart suggesting repulsive intermolecular interactions. However, heating to 620 K results in the creation of apparent block copolymers with a rigid rod−coil appearance, where the vast majority of the random coils, created by homocoupling of (**5**) are attached by at least one point to porphyrin **1** rods, Figure 8B(ii). The one-dimensional order in the porphyrin segment is maintained, with random chains of the perylene oligomer attached either at the sides or at the ends of rods, apparently growing away in all directions of the surface. Figure 8B(iii,iv) shows higher resolution STM data clearly indicating that the perylene units are in close contact at the end and side of a porphyrin **1** rod. For the individual perylene units attached to the side of a porphyrin **1** rod as shown in Figure 8B(iii), core-to-core molecular dimensions of 7.9 to 8.0 Å are observed, which are in agreement with the core-to-core distances of 8.1 and 8.5 Å calculated for porphyrin **1** connected by C−C bonds to the perylene long edge and the short edge, respectively. We also observe longer core-to-core distances of 10.5 Å in certain surface products such as that marked * in Figure 8B(i). In such instances bright protrusions between the connecting units are observed, suggesting that organometallic linkages may also occur between the two species.

## CONCLUSION

The coupling of different organic building blocks by a general surface-mediated intramolecular C−H bond-breaking and intermolecular bond-making mechanism has been demonstrated on a copper surface. Coupling *via* the C−H synthon provides a general approach to covalently link together many different organic entities at surfaces. Thus, a range of macromolecules is formed in parallel and selective ways, creating complexity and diversity from simple components. The individual chemistries used to prepare single component systems have been translated to multicomponent systems, a nontrivial result because different reactivities and relative rates of reactions has the potential to prevent bond formation between nonlike components. Further, we show that differences in C−H bond reactivity of individual components can be exploited in the deposition and heating protocols to tailor the outputs, *e.g.*, creating block polymers instead of random copolymers.

Overall, we demonstrate a simple "pick-mix-and-link" approach that enables the following aspects to be combined:

(i) We use the C−H bond as a generic synthon, which is ubiquitous in all organics and enables a wide range of cheap and accessible building blocks to be picked for on-surface synthesis. We have successfully used this approach for seven different organic components that are employed in molecular electronics, light harvesting and catalytic applications, and anticipate it can be translated to encompass a wide range of molecular building blocks.

(ii) We harness surface reactivity to activate many types of C−H bonds (porphyrinyl, arene, alkyl), demonstrating that readily available molecules are amenable for covalent linking at a surface. Our method generates complex organic heterostructures with ease, providing proof-of-principle that many different components can be coupled together at a surface.

(iii) We utilize the bond-making capability of a surface to create both C−C and C−metal−C covalent linkages, leading to facile generation of diverse macromolecules directly on the surface. The range of structures created are summarized in Figure 9, and link different functionalities and topologies together (rods, bricks, branches, coils); some of these structures are familiar from polymer syntheses, *e.g.*, branched ladder, the block polymer (guitar fret) or the rod−coil, but other combinations such as the "capped ladder", and the "key" are unique outputs of surface chemistry, and represent new classes of macromolecular entities that have no counterpart in organic synthesis.

(iv) In our systems, cleavage of the C−H bond only generates $H_2$ *via* recombinative desorption; *i.e.*, we achieve the linkage of organic components without depositing contamination on the surface; this is a significant achievement for device construction.

Finally, our approach demonstrates that on-surface synthesis using the C−H group as a synthon has the potential to emulate rapid discovery methods used in materials science[46−48] in which diverse and multivariate libraries of functional materials, possessing new combinations and arrangements of functional groups are generated, leading to improved or unexpected

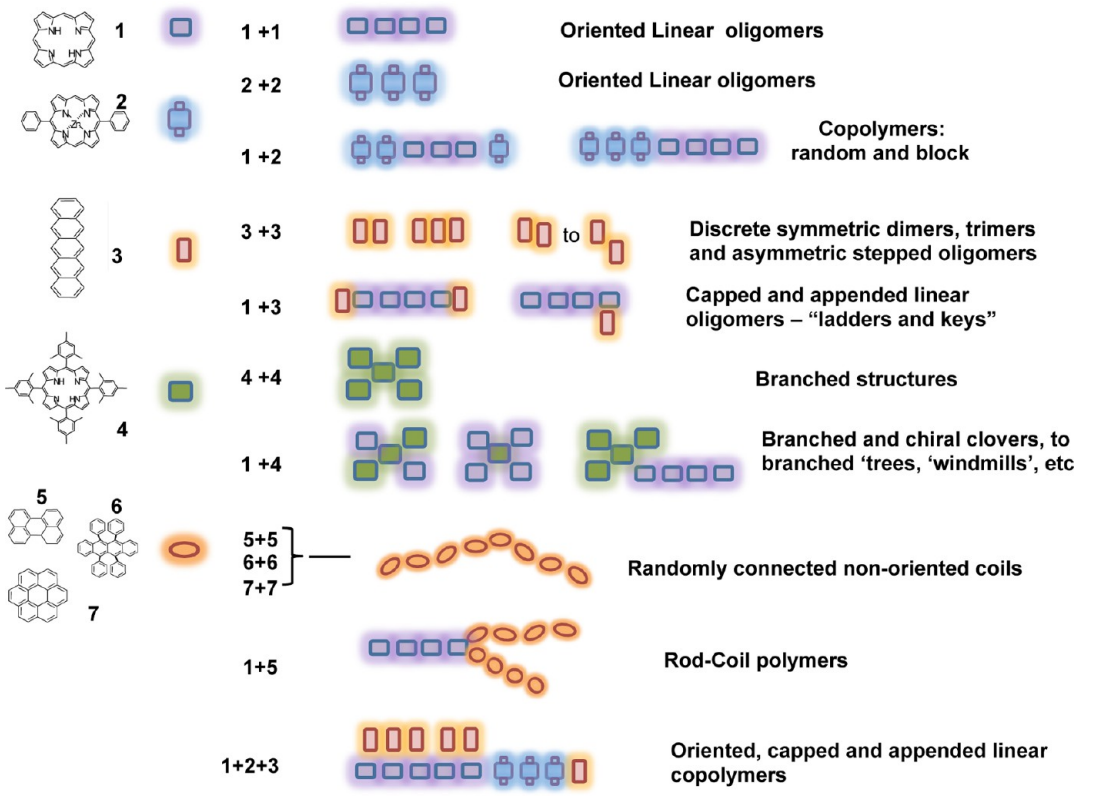


**Figure 9. Summary of molecules covalently linked on a Cu(110) surface in this study: 2*H*-porphyrin (1), Zn(II)-diphenylporphyrin (2), pentacene (3), tetramesitylporphyrin (4), perylene (5), rubrene (6) and coronene (7) with their associated chemical structures and the simplified schematic representations, which are used to illustrate the range of complex macromolecules formed.**

properties. Since the organic macromolecules and architectures required for viable surface-based molecular devices are largely unknown, we anticipate that our "pick-and-mix-and-link" approach at a surface will pave the way for generating large number of macromolecular products at a surface. Subsequent *in situ* screening of individual covalent structures for specific functions, such as nanomagnetism, conductance, sensing, reactivity, energy-transfer, and other molecular device attributes, can then be carried out using local probe techniques.[22,49] Once desired macromolecular structures are identified, the next step for the field is to direct the on-surface synthesis toward specific products while still retaining the C−H group as a synthon. This is a demanding future challenge for the field and will require consideration of a number of factors, some of which are highlighted below:

(i) As a first step, we have shown that it is possible to achieve control of on-surface macromolecular synthesis when required by exploiting the specific C−H reactivity encoded in each monomer. For example, the C−H bond reactivity of porphyrin **2** is greater than that of porphyrin **1**; by tailoring the deposition and heating conditions, we have demonstrated that the system can be driven either toward random copolymers or toward block copolymers. The concept of using the same synthon for different functional building blocks but utilizing designed protocols to achieve control of synthesis is novel in on-surface synthesis.

(ii) Second, activation of C−H bonds by the surface is dictated by a number of factors such as the adsorption geometry of the molecules, the spatial arrangements of molecular bonds with respect to the surface and the electronic/chemical effect of the surface on the molecule. Thus, tailoring of molecular structure alongside surface composition and geometry would enable specific C−H bond activation to be targeted. This, in fact, remains an outstanding challenge in heterogeneous catalysis.

(iii) Third, the surface-reactant and surface-product geometries also play a crucial role in determining which molecular building blocks may be reacted together, the nature of the intermolecular bonds that may be formed and the topology of the product on the surface. As an example, we show that the combination of surface and molecular symmetry and geometry determines the outcome of porphyrin coupling on the Cu(110) surface.[26,27] Homopolymers of porphyrin **1** and porphyrin **2** produce rod topologies that are perfectly aligned along the [001] direction of the surface, determined by the geometric match of the products with the surface. Thus, the porphyrin cores occupy specific adsorption positions, and the close commensurability of the C−Cu−C organometallic bonds with the underlying surface enables the

monomer−monomer distance to be bridged *via* accommodation of the connecting Cu atom near its favored 4-fold hollow sites. The geometric compatibility between porphyrin **1** and porphyrin **2** monomer units is also important in enabling a copolymer to be created. Similarly, pentacene also prefers to be adsorbed in a specific orientation with respect to the surface, in this case, with its long axis aligned along the [1$\bar{1}$0] direction. Pentacene dimers preserve this adsorption site preference, which is favorable for organometallic bonding, with the longer dimensions of the connecting C−Cu−C organometallic bonds able to bridge the distance between the two monomers and also position the connecting Cu atoms at their preferred 4-fold hollow sites. In contrast to the examples given above, tetramesitylporphyrin (**4**) connects *via* C−C linkages to give branched structures. We attribute this behavior to the fact that the molecule adopts a specific adsorption geometry at the surface in which the reactive 4-methyl groups are directed along specific diagonal directions. In this geometry, two adjacent porphyrin **4** entities can approach close enough to enable linking *via* the shorter C−C bond at the diagonal position, while still occupying their preferred adsorption sites.[25] The organometallic link is presumably not favored because suitable approach geometries which allow the monomers to occupy suitable adsorption sites, while maintaining an appropriate C−Cu−C distance in which connecting Cu atoms are positioned near their preferred 4-fold hollow sites, are not possible. Similarly, the nature of reactant-surface and product-surface geometry preferences and symmetry matching will also be expected to play an important role in determining that perylene on Cu(110) homocouples *via* C−C linkages and porphyrins on the 3-fold symmetric Ag(111) surface[50] react to form covalent carbon−carbon links between the meso and $\beta$ positions at the edges of the porphyrin ring. Therefore, it would appear that macromolecular product formation can be tuned as a function of both molecule and surface. However, *a priori* prediction of outcomes will require considerable theoretical development of complex molecule surface reaction mechanisms, a future need outlined recently by Bjork and Hanke.[51]

In conclusion, we have demonstrated that direct activation of C−H bonds intrinsic to $\pi$-functional molecules is a highly generic route for connecting different building blocks in different ways on a copper surface, enabling diverse macromolecules to be synthesized at a surface. Future advances in this field will require assaying individual heterostructures for function and, having identified successful architectures, to control C−H bond activation and intermolecular bond formation to create the desired products.

## METHODS

**Experimental Details.** STM experiments were performed at 300 K under ultrahigh vacuum (UHV) conditions using a Specs STM 150 Aarhus instrument. The STM was calibrated to better than 5% accuracy by measuring the atomic distances of the clean Cu(110) surface. All measurements were taken in constant current mode, using a tungsten tip and at a base pressure of $1.5 \times 10^{-10}$ mbar. Bias voltages are measured at the sample ($V = V_{sample}$). STM images were enhanced for brightness and contrast using the Image SxM program.[52] The Cu(110) surface was prepared in a UHV chamber using Argon ion sputtering and annealing cycles, and atomic flatness and cleanliness were checked by STM prior to dosing the molecule. $H_2$-porphyrin (**1**), and tetra(mesityl)porphyrin (**4**) (Frontier Scientific) and pentacene (**3**), perylene (**5**) (Sigma-Aldrich, all >98% purity) were used as purchased and sublimed onto the Cu(110) surface, which was held at room temperature during deposition. 5,15-Diphenylporphyrin was purchased from Frontier Scientific, and the zinc(II) complex was synthesized as described below.

**Synthesis.** The zinc(II) complex was synthesized by reaction with zinc(II)acetate in dimethylformamide at 120 °C for 3 h. The mixture was cooled and water was added. The precipitate was filtered, washed with water and diethyl ether and air-dried. The resulting material was chromatographed by flash column chromatography on silica using dichloromethane−hexane 4−6 as eluent. The product was further purified by crystallization from toluene. The product gave the characteristic spectroscopic data for this Zn(II)porphyrin[53] with no indication of the free base porphyrin in the UV−visible spectrum, laser desorption-ionization mass spectrum or in the $^1$H NMR spectrum.

**Computational Details.** All DFT calculations on pentacene-pentacene coupling in the gas phase were performed using the PBE density functional as implemented in the all electron numeric atomic orbital computational package FHI-aims.[54] All structures have been optimized using the FHI-aims tight basis set (atomic basis functions H: minimal basis + spspds, C: minimal basis + spdspdfg, Cu: minimal basis + spdfg), and until the maximal force on each atom was less than 0.01 eV/Å.

The DFT calculations of the Cu-connected pentacene on the Cu(110) surface were carried using version 5.2.12 of the VASP code.[55,56] A plane-wave basis set was used, with a cutoff energy of 400 eV. The optB86b van der Waals density functional was used,[57,58] with valence-core interactions included through the projector augmented wave method.[59] A 6 × 10 surface unit cell with 4 layers of Cu atoms and 3 nm of vacuum was used in the calculations of the adsorbed molecule. Of these, the bottom two were held fixed during the geometric relaxation of the system until forces on all the other atoms became less than 0.01 eV Å$^{-1}$. Gas phase calculations were carried out in a unit cell of dimensions 3 nm × 3 nm × 2 nm, in order to minimize interaction between periodic images. For all calculations the surface Brillouin zone was sampled only at the Γ-point. STM simulations were carried out using the Tersoff−Hammann approximation,[60,61] where the images were obtained from the local density of states integrated from the bias voltage to the Fermi level.

*Conflict of Interest:* The authors declare no competing financial interest.

*Acknowledgment.* The research was supported by the UK EPSRC Grant EP/F00981X/1 and EU ITN Project SMALL (Grant Agreement 238804) for R.R., the MINECO (Spain), under the Project CTQ2010-16339 and the Generalitat de Catalunya (Project 2009 SGR 158) for D.B.A., the EU Project ARTIST (Grant Agreement No. 243421) for F.H. and M.P., and EPSRC (EP/L000202) through MCC for computer resources at HECTOR for M.P.

*Supporting Information Available:* STM of pentacene on Cu(110) at 300 K showing diffusion. Theoretical modeling of pentacene−pentacene coupling in the gas-phase. Porphyrin−pentacene coupling at high coverage on Cu(110). Self-coupling

of rubrene and coronene on Cu(110). This material is available free of charge *via* the Internet at http://pubs.acs.org.

## REFERENCES AND NOTES


1. Ludlow, R. F.; Otto, S. Systems Chemistry. *Chem. Soc. Rev.* **2008**, *37*, 101–108.
2. Smits, E. C. P.; Mathijssen, S. G. J.; van Hal, P. A.; Setayesh, S.; Geuns, T. C. T.; Mutsaers, K. A. H. A.; Cantatore, E.; Wondergem, H. J.; Werzer, O.; Resel, R.; *et al.* Bottom-Up Organic Integrated Circuits. *Nature* **2008**, *455*, 956–959.
3. Aida, T.; Meijer, E. W.; Stupp, S. I. Functional Supramolecular Polymers. *Science* **2012**, *335*, 813–817.
4. Koepf, M.; Cherioux, F.; Wytko, J. A.; Weiss, J. 1D and 3D Surface-Assisted Self-Organization. *Coord. Chem. Rev.* **2012**, *256*, 2872–2892.
5. Grill, L.; Dyer, M.; Lafferentz, L.; Persson, M.; Peters, M. V.; Hecht, S. Nano-Architectures by Covalent Assembly of Molecular Building Blocks. *Nat. Nanotechnol.* **2007**, *2*, 687–691.
6. Weigelt, S.; Busse, C.; Bombis, C.; Knudsen, M. M.; Gothelf, K. V.; Lægsgaard, E.; Besenbacher, F.; Linderoth, T. R. Covalent Interlinking of an Aldehyde and an Amine on a Au(111) Surface in Ultrahigh Vacuum. *Angew. Chem., Int. Ed.* **2008**, *47*, 4406–4410.
7. Treier, M.; Fasel, R.; Champness, N. R.; Argent, S.; Richardson, N. V. Molecular Imaging of Polyimide Formation. *Phys. Chem. Chem. Phys.* **2009**, *11*, 1209–1214.
8. Jensen, S.; Fruchtl, H.; Baddeley, C. J. Coupling of Triamines with Diisocyanates on Au(111) Leads to the Formation of Polyurea Networks. *J. Am. Chem. Soc.* **2009**, *131*, 16706–16713.
9. Elemans, J. A. A. W.; Lei, S. B.; De Feyter, S. Molecular and Supramolecular Networks on Surfaces: From Two-Dimensional Crystal Engineering to Reactivity. *Angew. Chem., Int. Ed.* **2009**, *48*, 7298–7332.
10. Cai, J.; Ruffieux, P.; Jaafar, R.; Bieri, M.; Braun, T.; Blankenburg, S.; Matthias, M.; Seitsonen, A. P.; Saleh, M.; Feng, X.; *et al.* Atomically Precise Bottom-Up Fabrication of Graphene Nanoribbons. *Nature* **2010**, *466*, 470–473.
11. Matena, M.; Stöhr, M.; Riehm, T.; Björk, J.; Martens, S.; Dyer, M. S.; Persson, M.; Lobo-Checa, J.; Müller, K.; Enache, M.; *et al.* Aggregation and Contingent Metal/Surface Reactivity of 1,3,8,10-Tetraazaperopyrene (TAPP) on Cu(111). *Chem.—Eur. J.* **2010**, *16*, 2079–2091.
12. Bartels, L. Tailoring Molecular Layers at Metal Surfaces. *Nat. Chem.* **2010**, *2*, 87–95.
13. Lipton-Duffin, J. A.; Miwa, J. A.; Kondratenko, M.; Cicoira, F.; Sumpter, B. G.; Meunier, V.; Perepichka, D. F.; Rosei, F. Step-by-Step Growth of Epitaxially Aligned Polythiophene by Surface-Confined Reaction. *Proc. Natl. Acad. Sci. U. S. A.* **2010**, *107*, 11200–11204.
14. Abel, M.; Clair, S.; Ourdjini, O.; Mossoyan, M.; Porte, L. Single Layer of Polymeric Fe-Phthalocyanine: An Organometallic Sheet on Metal and Thin Insulating Film. *J. Am. Chem. Soc.* **2011**, *133*, 1203–1205.
15. Lackinger, M.; Heckl, W. M. A STM Perspective on Covalent Intermolecular Coupling Reactions on Surfaces. *J. Phys. D: Appl. Phys.* **2011**, *44*, 464011.
16. Lafferentz, L.; Eberhardt, V.; Dri, C.; Africh, C.; Comelli, G.; Esch, F.; Hecht, S.; Grill, L. Controlling On-Surface Polymerization by Hierarchical and Substrate-Directed Growth. *Nat. Chem.* **2012**, *4*, 215–220.
17. Tanoue, R.; Higuchi, R.; Ikebe, K.; Uemura, S.; Kimizuka, N.; Stieg, A. Z.; Gimzewski, J. K.; Kunitake, M. *In Situ* STM Investigation of Aromatic Poly(azomethine) Arrays Constructed by "On-Site" Equilibrium Polymerization. *Langmuir* **2012**, *28*, 13844–13851.
18. Greenwood, J.; Fruechtl, H. A.; Baddeley, C. J. Surface-Confined Reaction of Aliphatic Diamines with Aromatic Diisocyanates on Au{111} Leads to Ordered Oligomer Assemblies. *J. Phys. Chem. C* **2013**, *117*, 4515–4520.
19. Sun, Q.; Zhang, C.; Li, Z.; Kong, H.; Tan, Q.; Hu, A.; Xu, W. On-Surface Formation of One-Dimensional Polyphenylene Through Bergman Cyclization. *J. Am. Chem. Soc.* **2013**, *135*, 8448–8451.
20. Treier, M.; Pignedoli, C. A.; Laino, T.; Rieger, R.; Mullen, K.; Passerone, D.; Fasel, R. Surface-Assisted Cyclodehydrogenation Provides a Synthetic Route Towards Easily Processable and Chemically Tailored Nanographenes. *Nat. Chem.* **2011**, *3*, 61–67.
21. Dinca, L. E.; Fu, C. Y.; MacLeod, J. M.; Lipton-Duffin, J.; Brusso, J. L.; Szakacs, C. E.; Ma, D. L.; Perepichka, D. F.; Rosei, F. Unprecedented Transformation of Tetrathienoanthracene into Pentacene on Ni(111). *ACS Nano* **2013**, *7*, 1652–1657.
22. DiLullo, A.; Chang, S. H.; Baadji, N.; Clark, K.; Klockner, J. P.; Prosenc, M. H.; Sanvito, S.; Wiesendanger, R.; Hoffmann, G.; Hla, S. W. Molecular Kondo Chain. *Nano Lett.* **2012**, *12*, 3174.
23. Xiang, D.; Sun, X.; Briceño, G.; Lou, Y.; Wang, K. A.; Chang, H.; Wallace-Freedman, W. G.; Chen, S. W.; Schultz, P. G. A Combinatorial Approach to Materials Discovery. *Science* **1995**, *268*, 1738–1740.
24. Stoddart, J. F. Thither Supramolecular Chemistry? *Nat. Chem.* **2009**, *1*, 14–15.
25. In't Veld, M.; Iavicoli, P.; Haq, S.; Amabilino, D. B.; Raval, R. Unique Intermolecular Reaction of Simple Porphyrins at a Metal Surface Gives Covalent Nanostructures. *Chem. Commun.* **2008**, 1536–1538.
26. Haq, S.; Hanke, F.; Dyer, M. S.; Persson, M.; Iavicoli, P.; Amabilino, D. B.; Raval, R. Clean Coupling of Unfunctionalized Porphyrins at Surfaces To Give Highly Oriented Organometallic Oligomers. *J. Am. Chem. Soc.* **2011**, *133*, 12031–12039.
27. Hanke, F.; Haq, S.; Raval, R.; Persson, M. Heat to Connect: Surface Commensurability Directs Covalent One-Dimensional Self-Assembly. *ACS Nano* **2011**, *5*, 9093–9103.
28. Ditze, S.; Stark, M.; Drost, M.; Buchner, F.; Steinruck, H. P.; Marbach, H. Activation Energy for the Self-Metalation Reaction of 2*H*-Tetraphenylporphyrin on Cu(111). *Angew. Chem., Int. Ed.* **2012**, *51*, 10898–10901.
29. Goldoni, A.; Pignedoli, C. A.; Di Santo, G.; Castellarin-Cudia, C.; Magnano, E.; Bondino, F.; Verdini, A.; Passerone, D. Room Temperature Metalation of 2*H*-TPP Monolayer on Iron and Nickel Surfaces by Picking up Substrate Metal Atoms. *ACS Nano* **2012**, *6*, 10800–10807.
30. Davies, H. M. L.; Du Bois, J.; Yu, J.-Q. C−H Functionalization in Organic Synthesis. *Chem. Soc. Rev.* **2011**, *40*, 1855–1856.
31. Siaj, M.; McBreen, P. H. Creating, Varying, and Growing Single-Site Molecular Contacts. *Science* **2005**, *309*, 588–590.
32. Carroll, R. L.; Gorman, C. B. The Genesis of Molecular Electronics. *Angew. Chem., Int. Ed.* **2002**, *41*, 4378–4400.
33. Dyer, M. S.; Robin, A.; Haq, S.; Raval, R.; Persson, M.; Klimes, J. Understanding the Interaction of the Porphyrin Macrocycle to Reactive Metal Substrates: Structure, Bonding, and Adatom Capture. *ACS Nano* **2011**, *5*, 1831–1838.
34. Lehnherr, D.; Tykwinski, R. R. Oligomers and Polymers Based on Pentacene Building Blocks. *Materials* **2010**, *3*, 2772–2800.
35. Müller, K.; Kara, A.; Kim, T. K.; Bertschinger, R.; Scheybal, A.; Osterwalder, J.; Jung, T. A. Multimorphism in Molecular Monolayers: Pentacene on Cu(110). *Phys. Rev. B: Condens. Matter Mater. Phys.* **2009**, *79*, 245421.
36. Müller, K.; Seitsonen, A. P.; Brugger, T.; Westover, J.; Greber, T.; Jung, T.; Kara, A. Electronic Structure of an Organic/Metal Interface: Pentacene/Cu(110). *J. Phys. Chem. C* **2012**, *116*, 23465–23471.
37. Bieri, M.; Nguyen, M. T.; Groning, O.; Cai, J. M.; Treier, M.; Ait-Mansour, K.; Ruffieux, P.; Pignedoli, C. A.; Passerone, D.; Kastler, M.; *et al.* Two-Dimensional Polymer Formation on Surfaces: Insight into the Roles of Precursor Mobility and Reactivity. *J. Am. Chem. Soc.* **2010**, *132*, 16669–16676.
38. Ditze, S.; Rockert, M.; Buchner, F.; Zillner, E.; Stark, M.; Steinruck, H. P.; Marbach, H. Towards the Engineering of Molecular Nanostructures: Local Anchoring and Functionalization of Porphyrins on Model-Templates. *Nanotechnology* **2013**, *24*, 115305.
39. J. Björk, J.; Matena, M.; Dyer, M. S.; Enache, M.; Lobo-Checa, J.; Gade, L. H.; Jung, T. A.; Stöhr, M.; Persson, M. STM Fingerprint of Molecule-Adatom Interactions in a Self-Assembled

Metal-Organic Surface Coordination N on Cu(111). *Phys. Chem. Chem. Phys.* **2010**, *12*, 8815.
40. Lin, N.; Dmitriev, A.; Weckesser, J.; Barth, J. V.; Kern, K. Real-Time Single-Molecule Imaging of the Formation and Dynamics of Coordination Compounds. *Angew. Chem., Int. Ed.* **2002**, *41*, 4779–4783.
41. Dong, L.; Sun, Q.; Zhang, C.; Li, Z. W.; Sheng, K.; Kong, H. H.; Tan, Q. G.; Pan, Y. X.; Hu, A. G.; Xu, W. A Self-Assembled Molecular Nanostructure for Trapping the Native Adatoms on Cu(110). *Chem. Commun.* **2013**, *49*, 1735–1737.
42. Fan, Q. T.; Wang, C. C.; Han, Y.; Zhu, J. F.; Kuttner, J.; Hilt, G.; Gottfried, J. M. Surface-Assisted Formation, Assembly, and Dynamics of Planar Organometallic Macrocycles and Zigzag Shaped Polymer Chains with C-Cu-C Bonds. *ACS Nano* **2014**, *8*, 709–718.
43. Luo, J.; Xu, M.; Li, R.; Huang, K. W.; Jiang, C.; Qi, O.; Zeng, W.; Zhang, J.; Chi, C.; Wang, P.; Wu, J. N-Annulated Perylene as An Efficient Electron Donor for Porphyrin-Based Dyes: Enhanced Light-Harvesting Ability and High-Efficiency Co(II/III)-Based Dye-Sensitized Solar Cells. *J. Am. Chem. Soc.* **2014**, *136*, 265–272.
44. Witte, G.; Hanel, K.; Busse, C.; Birkner, A.; Woll, C. Molecules Coining Patterns into a Metal: The Hard Core of Soft Matter. *Chem. Mater.* **2007**, *19*, 4228–4233.
45. Pinardi, A. L.; Otero-Irurueta, G.; Palacio, I.; Martinez, J. I.; Sanchez-Sanchez, C.; Tello, M.; Rogero, C.; Cossaro, A.; Preobrajenski, A.; Gómez-Lor, B.; *et al.* Tailored Formation of N-Doped Nanoarchitectures by Diffusion-Controlled On-Surface (Cyclo)Dehydrogenation of Heteroaromatics. *ACS Nano* **2012**, *7*, 3676–3684.
46. Jones, J. T. A.; Hasell, T.; Wu, X. F.; Bacsa, J.; Jelfs, K. E.; Schmidtmann, M.; Chong, S. Y.; Adams, D. J.; Trewin, A.; Schiffman, F.; *et al.* Modular and Predictable Assembly of Porous Organic Molecular Crystals. *Nature* **2011**, *474*, 367–371.
47. Zhu, Z. X.; Cardin, C. J.; Gan, Y.; Colquhoun, H. M. Sequence-Selective Assembly of Tweezer Molecules on Linear Templates Enables Frameshift-Reading of Sequence Information. *Nat. Chem.* **2010**, *2*, 653–660.
48. Deng, H.; Doonan, C. J.; Furukawa, H.; Ferreira, R. B.; Towne, J.; Knobler, C. B.; Wang, B.; Yaghi, O. M. Multiple Functional Groups of Varying Ratios in Metal-Organic Frameworks. *Science* **2010**, *327*, 846–850.
49. Lafferentz, L.; Ample, F.; Yu, H.; Hecht, S.; Joachim, C.; Grill, L. Conductance of a Single Conjugated Polymer As a Continuous Function of its Length. *Science* **2009**, *323*, 1193–1197.
50. Wiengarten, A.; Seufert, K.; Auwärter, W.; Ecija, D.; Diller, K.; Allegretti, F.; Bischoff, F.; Fischer, S.; Duncan, D. A.; Papageorgiou, A. C.; *et al.* Surface-Assisted Dehydrogenative Homocoupling of Porphine Molecules. *J. Am. Chem. Soc.* **2014**, *136*, 9346–9354.
51. Björk, J.; Hanke, F. Towards Design Rules for Covalent Nanostructures on Metal Surfaces. *Chem.—Eur. J.* **2014**, *20*, 928–934.
52. Barrett, S. D. *Image SXM*; University of Liverpool: Liverpool, U.K., 2012; http://www.ImageSXM.org.uk.
53. Lin, V. S. Y.; Iovine, P. M.; DiMagno, S. G.; Therien, M. J. Dipyrryl and Porphyrinic Precursors to Supramolecular Conjugated (Porphinato)Metal Arrays: Synthesis of Dipyrrylmethane and (5,15-Diphenylporphinato)zinc(II). *Inorg. Synth.* **2002**, *33*, 55–61.
54. Perdew, J. P.; Burke, K.; Ernzerhof, M. Generalized Gradient Approximation Made Simple. *Phys. Rev. Lett.* **1996**, *77*, 3865–3868.
55. Kresse, G.; Furthmüller, J. Efficient Iterative Schemes for *AB Initio* Total-Energy Calculations Using a Plane-Wave Basis Set. *Phys. Rev. B: Condens. Matter Mater. Phys.* **1996**, *54*, 11169–11186.
56. Kresse, G.; Furthmüller, J. Efficiency of *Ab-Initio* Total Energy Calculations for Metals and Semiconductors Using a Plane-Wave B Set. *Comput. Mater. Sci.* **1996**, *6*, 15–50.
57. Klimeš, J.; Bowler, D. R.; Michaelides, A. Chemical Accuracy for the Van der Waals Density Functional. *J. Phys.: Condens. Matter* **2010**, *22*, 022201.
58. Klimeš, J.; Bowler, D. R.; Michaelides, A. Van der Waals Density Functionals Applied to Solids. *Phys. Rev. B: Condens. Matter Mater. Phys.* **2011**, *83*, 195131.
59. Kresse, G.; Joubert, D. From Ultrasoft Pseudopotentials to the Projector Augmented-Wave Method. *Phys. Rev. B: Condens. Matter Mater. Phys.* **1999**, *59*, 1758–1775.
60. Tersoff, J.; Hamann, D. R. Theory and Application for the Scanning Tunneling Microscope. *Phys. Rev. Lett.* **1983**, *50*, 1998–2001.
61. Tersoff, J.; Hamann, D. R. Theory of The Scanning Tunneling Microscope. *Phys. Rev. B: Condens. Matter Mater. Phys.* **1985**, *31*, 805–813.